JOURNAL OF APPLIED ELECTROCHEMISTRY 25 (1995) 450–455

Mass transport to reticulated vitreous carbon rotating cylinder electrodes

A. H. NAHLÉ*, G. W. READE, F. C. WALSH‡

Division of Chemistry, School of Chemistry, Physics & Radiography, University of Portsmouth, White Swan Road, Portsmouth PO1 2DT, Great Britain

Received 21 April 1994; revised 12 October 1994

Mass transport to rotating cylinder electrodes (radius 0.5 cm and height 1.2 cm) fabricated from reticulated vitreous carbon (RVCRCE) was investigated using linear sweep voltammetry in a 0.5 M Na_2SO_4 + 1 mM $CuSO_4$ electrolyte at pH 2. At a fixed cupric ion concentration the limiting current was found to be dependent upon velocity to the power 0.55 to 0.71 depending upon the porosity grade of the carbon foam. The product of mass transport coefficient and specific electrode area, $k_m A_e$, was found to be approximately 0.51 s^{-1} at 157 rad s^{-1} (corresponding to 1500 rpm) for the 100 ppi material. The experimental data are compared to the predicted performance of a hydrodynamically smooth rotating disc electrode (RDE) and rotating cylinder electrode (RCE).

Nomenclature

A	electrode area (cm^2)
A_e	active electrode area per unit volume (cm^{-1})
c_B	bulk copper concentration (mol cm^{-3})
c_0	concentration at $t = 0$ (mol cm^{-3})
c_t	concentration at time t (mol cm^{-3})
D	diffusion coefficient ($cm^2 s^{-1}$)
F	Faraday constant (96 485 A s mol^{-1})
h	height of rotating cylinder electrode (cm)
I_L	limiting current (A)
$I_{L,RDE}$	limiting current at an RDE (A)
$I_{L,RCE}$	limiting current at an RCE (A)
$I_{L,RVC}$	limiting current at a rotating RVCRCE (A)
k_m	mass transport coefficient (cm s^{-1})
r	radius of RCE (cm)
U	electrolyte velocity (cm s^{-1})
V	reactor volume (cm^3)
V_e	overall volume of electrode (cm^3)
x	characteristic length (cm)
z	number of electrons

Greek symbols

β	ratio of limiting current at an RVCRCE relative to an RDE of same diameter
γ	ratio of limiting current at an RVCRCE relative to an RCE of same overall volume
δ	thickness of the diffusion layer (cm)
ν	electrolyte viscosity ($cm^2 s^{-1}$)
ω	rotation speed (rad s^{-1})

Dimensionless groups

$Re = Ux/\nu$	Reynolds number
$Sc = \nu/D$	Schmidt number
$Sh = k_m x/D$	Sherwood number

1. Introduction

Rotating disc electrodes [1] and rotating cylinder electrodes [2] are well established as controlled flow electrodes for kinetic and analytical applications. The RDE is used almost exclusively in the laboratory while the RCE has been used extensively in industrial applications for the removal of metal ions from effluents [3].

Reticulated vitreous carbon (RVC) electrodes have been in use for over a decade. The majority of earlier work has concerned the use of static electrodes for analytical applications [4–8]. These papers have shown that RVC electrodes are capable of very high analytical sensitivity although high background noise can be problematic at low reactant concentrations.

A rotating RVC electrode was developed by Blaedel and Wang to help overcome problems with background noise [9]. To achieve this they demonstrated the use of pulse rotation voltammetry in conjunction with differential pulse anodic stripping voltammetry. Using ferricyanide reduction in 0.1 M phosphate buffer they found that the limiting current was dependent upon rotation speed to the power 0.508 for a squat cylinder of radius 2.7 mm and height 2.2 mm. Following this, the same authors reported the design of a flow through analytical detector utilising a rotating squat RVC cylinder electrode [10]

* Permanent address: Chemistry Department, Faculty of Arts and Sciences, The American University of Beirut, The Lebanon.
‡ Author to whom all correspondence should be addressed.

0021-891X 1995 Chapman & Hall

and reported results using cylinders of radius 2 mm and heights of 1.8 mm and 8.4 mm. For the cylinder of smaller height they found a dependence of limiting current upon rotation speed to the power 0.47. Although data for the dependence of limiting current upon rotation speed are presented for the 8.4 mm cylinder, the authors discovered that below flow rates of 1 $cm^3\ min^{-1}$ steady state limiting currents were not achieved. These observations were attributed to very fast depletion of the electroactive species, that is, to a high fractional conversion over the detector.

RVC electrodes have also found use as substrates for metal deposits. For example, work has been published describing the use of a mercury-plated RVC electrode, in the form of a flow through 100 ppi disc of radius 0.55 cm and 0.24 cm depth, for use in anodic stripping voltammetry. Blaedel and Wang have reported detected capabilities down to 3×10^{-9} M of cadmium, copper, lead and zinc ions in acetate buffer at pH 4.8 for deposition times of up to five minutes [11].

Heider *et al.* have used an RVC electrode partially plated with platinum as an improved biosensor for glucose determination [12]. They showed that glucose oxidase may be immobilized on the glassy carbon surface whilst the platinum provides an enhanced response to hydrogen peroxide oxidation. Zamponi, Marrassi and other coworkers have reported the use of a gold plated RVC electrode in an OTTLE cell [14]. It was found that the fast and efficient electrolyses at these electrodes were due to the increased surface area produced by a crystalline deposit of gold.

In another paper Zamponi *et al.* have reported the use of a mercury-plated rotating RVC (100 ppi) electrode of 0.27 cm radius and 0.22 cm depth for anodic stripping voltammetry [14]. An enhanced response of approximately 60 times was found in electrolytes containing 40 $\mu g\ dm^{-3}$ Cd(II) and Pb(II) for this electrode when compared with a smooth mercury plated glassy carbon electrode.

Three recent papers have illustrated the use of an RVC flow-through reactor in a batch recirculation [15, 16] and single pass [17] mode for the removal of metal ions down to the sub ppm level. The work also reported the effects of the presence of oxygen in the system and the results show that current efficiencies can be maintained at a relatively high level even at low metal ion concentrations under correct potentiostatic control.

The aim of the present study is to quantify the space averaged mass transport to a rotating RVC cylinder electrode (RVCRCE). In order to provide a working comparison the RVCRCEs are compared to an RDE of the same radius as the RVCRCE and also to an RCE of the same diameter and length.

2. Mass transport expressions

If it is assumed that the reactant concentration is spatially invariant (due to effective mixing of the electrolyte) the limiting current at a two dimensional electrode may be expressed in terms of the averaged mass transport coefficient, k_m, and the active electrode area, A, via the expression

$$I_L = k_m A z F c_B \tag{1}$$

It has been noted elsewhere [19] that the factor $k_m A$ is a useful guide for reactor comparison. The limiting current is given by the Levich equation [1] for a hydrodynamically smooth RDE rotating in an infinite container:

$$I_{L,RDE} = 0.62 z F A c_B D^{2/3} \nu^{-1/6} \omega^{1/2} \tag{2}$$

Mass transport characteristics may be determined via the use of dimensionless group correlations such as

$$Sh = aRe^b Sc^c \tag{3}$$

where the Sh and Re numbers can be defined in terms of, for example, the radius or the diameter of the rotating electrode as the characteristic length. For rotating systems it is common to define a 'rotational' Reynolds number so that

$$Re = \frac{\omega r x}{\nu} \tag{4}$$

Eisenberg, Tobias and Wilke [19] used a Reynolds number based on the diameter of the RCE

$$Re_d = \frac{2\omega r^2}{\nu} \tag{5}$$

to characterize the mass transport to a hydrodynamically smooth RCE under a wide range of electrolyte conditions. Allowing for a change from the Stanton number correlation used in [19] to a Sherwood number expression, the mass transport correlation for a hydrodynamically smooth RCE can be written as follows:

$$Sh_d = 0.079 Re_d^{0.70} Sc^{0.356} \tag{6}$$

If the Sherwood and Reynolds numbers are written in terms of the radius of the RCE as the characteristic length, Equation 6 becomes:

$$Sh_r = 0.064 Re_r^{0.70} Sc^{0.356} \tag{7}$$

This correlation may be rewritten as an expression for the limiting current at a hydrodynamically smooth RCE in terms of the RCE radius:

$$I_{L,RCE} = 0.064 z F A c_B D^{0.64} \nu^{-0.34} \omega^{0.70} r^{0.40} \tag{8}$$

Here, a porous electrode of fixed volume ($V_e = 0.942\ cm^3$) is studied and the limiting current may be expressed as

$$I_L = k_m A_e V_e z F c_B \tag{9}$$

The bulk concentration of cupric ions, c_B, is maintained at a constant value here by the use of a soluble anode and a well mixed electrolyte.

3. Experimental details

The electrode (Fig. 1) consisted of a porous cylinder ($r = 0.5$ cm, $h = 1.2$ cm) bored from a 12 mm thick RVC sheet [20] using a hollow cylindrical tool. The

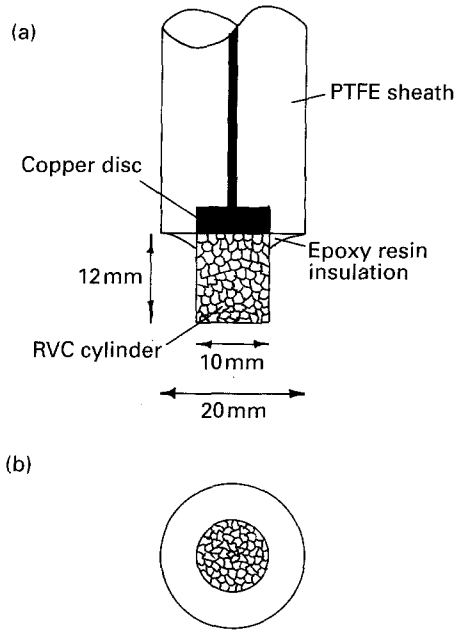

Fig. 1. RVC rotating cylinder electrode: (a) sectional view; (b) plan.

RVC cylinder was cemented to a copper RDE using a conducting glue (RS Components silver-loaded epoxy resin) followed by stoving at 80 °C for 2 h. 100 and 60 ppi RVC cylinder electrodes of differing heights ($r = 0.5$ cm) were machined to size on a lathe. The silver at the base of the electrode was masked off with a quick setting insulating adhesive (Ciba Geigy 2001 epoxy resin). The three electrode, two compartment glass cell shown in Fig. 2 was used. The counter electrode was a copper foil (Fisons) and was placed around the walls of the working electrode compartment. Auxiliary experiments showed that the copper anode dissolved with unity current efficiency and the bulk concentration was shown to be constant throughout the experiments by the use of atomic absorption spectrophotometric analysis.

Linear sweep voltammetry was carried out using a Thompson electrochemistry rotating disc electrode system in conjunction with a Hi-Tek Instruments DT 2101 potentiostat and a Hi-Tek Instruments PPRI wave form generator. The current versus potential curves were recorded on a Bryans 26000 X–Y recorder.

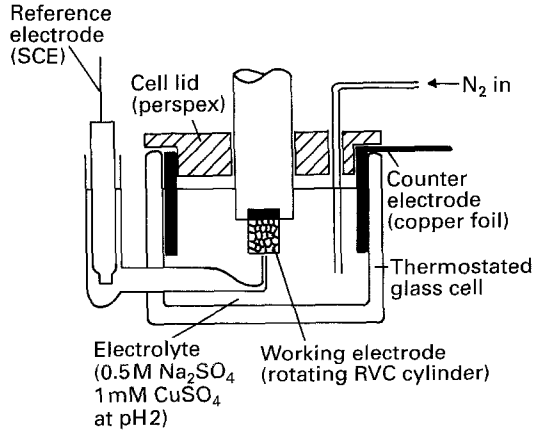

Fig. 2. Schematic of the rotating electrode cell.

Table 1. Electrolyte characteristics

Background electrolyte	0.5 M sodium sulphate adjusted to pH 2
Electroactive species	1 mM copper sulphate
Viscosity	0.0117 $cm^2 s^{-1}$
Diffusion coefficient	4.9×10^{-6} $cm^2 s^{-1}$
Schmidt number	2388
Temperature	25 ± 0.5 °C

The electrolyte used in all cases was 0.001 M copper sulphate (May and Baker AR grade) in 0.5 M sodium sulphate adjusted to pH 2 with sulphuric acid (see Table 1). Solutions were prepared volumetrically and the total copper concentration was measured using atomic absorption spectroscopy. The electrolyte was degassed with a fast stream of nitrogen and thermostated to 25 ± 0.5 °C. Prior to use, the electrode was rinsed in acetone followed by doubly-distilled water then by a second acetone rinse. The final acetone rinse (immediately before use) served to ensure that the void volume within the electrode contained no entrapped air.

The RVC electrode was swept from the open circuit potential (typically +54 mV vs SCE) to a value of −850 mV vs SCE and the current against potential curve was then recorded at a sweep rate of 5 mV s^{-1}. At the end of the potential sweep, the electrode was pulsed to +500 mV vs SCE to remove the copper. Once the current had reached a steady value, the electrolyte was replaced and the procedure was repeated for a different rotation speed. In this way the current against potential curves were recorded between 26.2 and 262 rad s^{-1} (corresponding to 250 and 2500 rpm). After each set of rotation speeds the electrode was replaced by a new one. Four grades of RVC were employed in this set of experiments (i.e., 10, 30, 60 and 100 pores per linear inch (ppi)).

4. Results and discussion

Figure 3 shows a typical set of current voltage curves, in this case for the 10 ppi electrode and the estimated

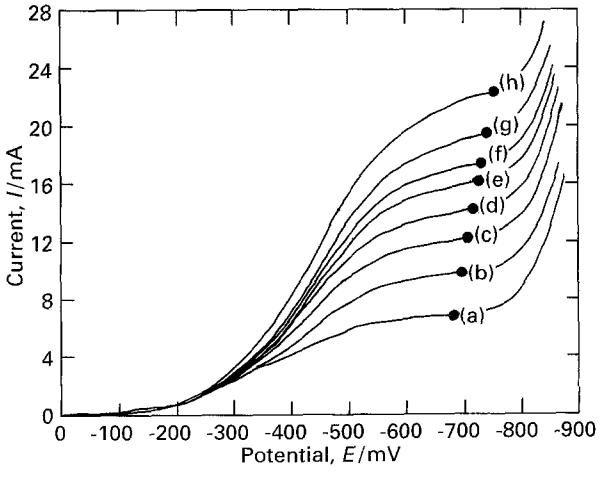

Fig. 3. Current against potential curves for the 10 ppi rotating RVC cylinder electrode. (a) 26.2, (b) 52.4, (c) 78.5, (d) 104.7, (e) 130.9, (f) 157.1, (g) 183.3 and (h) 209.4 rad s^{-1}. Corresponding to 250 rpm increments between 250 and 2000 rpm. The solid circles show the estimated limiting current values.

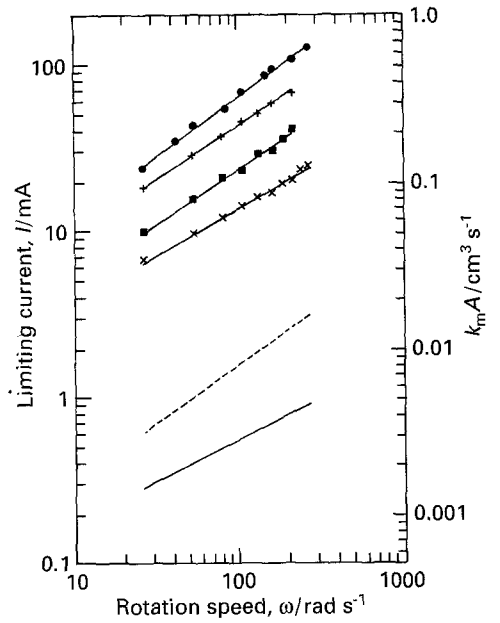

Fig. 4. Logarithmic plot of limiting current versus rotation speed for the four grades of rotating RVC cylinder electrode ($h = 1.2$ cm, $r = 0.5$ cm). Key: (×) 10 ppi, (■) 30 ppi, (+) 60 ppi and (●) 100 ppi. The vertical axis also shows the product of the mass transport coefficient and the electrode area, $k_m A$. The solid and broken lines show the predicted performance for a smooth RDE having the same diameter and a smooth RCE having the same diameter and length.

limiting current values are indicated. At higher speeds the plateau contracts and at 26.2 rad s^{-1} (corresponding to 250 rpm) the limiting current region appears as an inflection over a potential range of less than 200 mV. At this rotation speed the half wave potential occurs at approximately −345 mV vs SCE. As the rotation speed increases the half wave potential shifts negatively (approximately −425 mV vs SCE at 262 rad s^{-1}) and the curves develop a slope in the limiting current 'plateau' region. This behaviour may be attributed to both rough copper deposition and a significant degree of uncompensated *IR*-drop in the system. Figure 4 shows a double logarithmic plot of limiting current versus rotation speed for the four grades of RVC. Also shown are the predicted limiting currents against rotation speed for the comparable RDE (Equation 2) and RCE (Equation 8). The slopes of the graphs were calculated using linear least squares regression resulting in the equations of the lines and their correlation coefficients shown in Table 2 according to the following equation:

$$I_L = K\omega^n \tag{10}$$

The experimental limiting current values may be

Table 2. Line equations and least squares regression correlation coefficients for the four grades of RVC
Based upon limiting current versus rotation speed data.

RVC grade/ppi	*Line equation*	*Correlation coefficient*
10	$I_L = 0.0012\omega^{0.55}$	0.996
30	$I_L = 0.0011\omega^{0.66}$	0.996
60	$I_L = 0.0023\omega^{0.63}$	0.999
100	$I_L = 0.0024\omega^{0.71}$	0.998

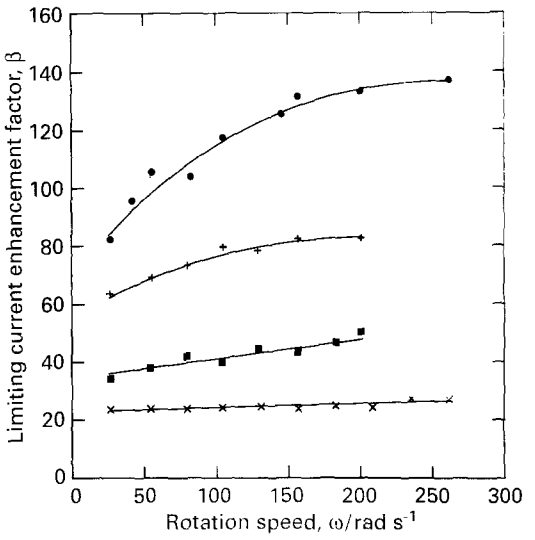

Fig. 5. Plot of the limiting current enhancement factor β against rotation speed for the four grades of rotating RVC cylinder electrode. $\beta = 1$ corresponds to the limiting current at a smooth RDE of the same radius as the RVC cylinder. Key: (×) 10 ppi, (■) 30 ppi, (+) 60 ppi and (●) 100 ppi.

compared to theoretical limiting current values for the hydrodynamically smooth RDE and RCE by defining dimensionless limiting current enhancement factors β and γ defined as

$$\beta = \frac{I_{L,RVC}}{I_{L,RDE}} \tag{11}$$

and

$$\gamma = \frac{I_{L,RVC}}{I_{L,RCE}} \tag{12}$$

These are effectively mass transport enhancement factors based upon the limiting current.

Figures 5 and 6 show plots of the limiting current based enhancement factors versus rotation speed for the four grades of foam. The RVCRCEs show

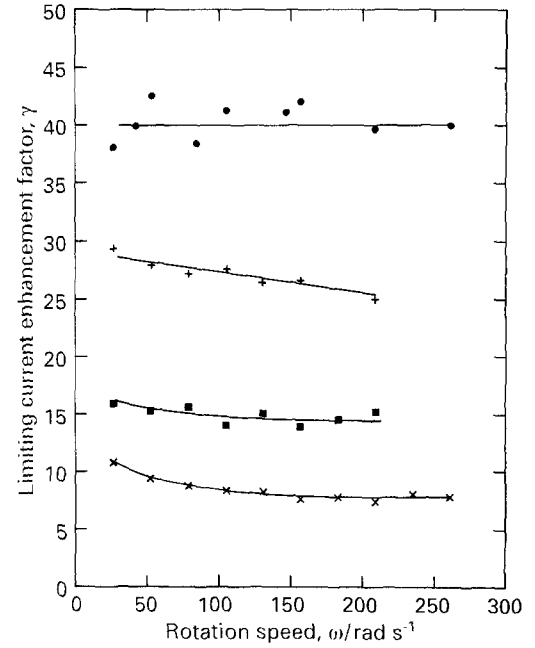

Fig. 6. Plot of the limiting current enhancement factor γ against rotation speed for the four grades of rotating RVC cylinder electrode. Key: (×) 10 ppi, (■) 30 ppi, (+) 60 ppi and (●) 100 ppi. $\gamma = 1$ corresponds to the limiting current at a smooth RCE of the same overall volume as the RVC cylinder.

Table 3. Electroactive area per unit volume for the four grades of RVC

RVC grade/ppi	A_e/cm^{-1}	A_eV_e/cm^2	*Reference*
10	13.5 ± 1.5	12.7	[22]
30	24.6 ± 2.0	23.2	[22]
60	37.5	35.3	[21]
100	67.5 ± 1.0	63.6	[22]

limiting current enhancements of between 20 times (10 ppi) to over 130 times (100 ppi) when compared to the RDE. Enhancements of approximately 7 to 40 times are seen for the RVCRCEs when compared to the RCE. The difference in the shape of the plots in Fig. 5 along with the differing slopes seen at the RVCRCEs suggests a change in the mass transport conditions for the different grades of foam. The data for the 100 ppi cylinder in Fig. 6 do not show a good correlation with rotation speed highlighting possible changes in the flow regime within the porous matrix.

Transforming β and γ into enhancement factors based upon the product of mass transport coefficient and electrode area results in the following equations:

$$\beta = \frac{(k_m A_e V_e)_{RVC}}{(k_m A)_{RDE}} \tag{13}$$

$$\gamma = \frac{(k_m A_e V_e)_{RVC}}{(k_m A)_{RCE}} \tag{14}$$

A knowledge of A_e (see Table 3) allows a relative mass transport coefficient to be expressed as

$$\beta' = \frac{k_{m,RVC}}{k_{m,RDE}} \tag{15}$$

and

$$\gamma' = \frac{k_{m,RVC}}{k_{m,RCE}} \tag{16}$$

It is found that, for the four RVCRCEs, the values for β' lie in the range 1 to 1.85. This leads to the conclusion that the mass transport coefficients to the RVCRCEs are of the same order of magnitude as the RDE in accordance with the findings of Blaedel and Wang [9].

Experiments were performed using two other different heights of 100 ppi RVCRCE ($h = 0.9$ cm and 0.5 cm) at constant radius of 0.5 cm. The data are shown in Fig. 7 in the form of a logarithmic plot of (I_L/V_e) against rotation speed. The slopes of the log limiting current against log rotation speed plots for the 0.9 cm and 0.5 cm high RVCRCE are 0.62 and 0.58, respectively; the correlation coefficients are

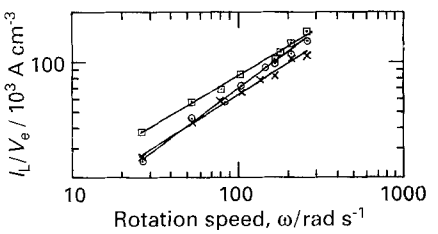

Fig. 7. Logarithmic plot of (I_L/V_e) against rotation speed for three heights of 100 ppi grade of rotating RVC cylinder. (□) 0.5 cm high, (○) 1.2 cm high and (×) 0.9 cm high.

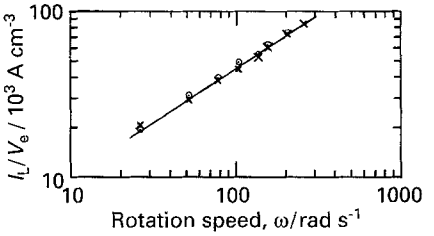

Fig. 8. Logarithmic plot of (I_L/V_e) against rotation speed for two heights of 60 ppi RVC cylinder electrode. (○) 1.2 cm high and (×) 0.9 cm high.

both greater than 0.995. As can be seen from Fig. 7, the 1.2 cm and 0.9 cm RVCRCEs exhibit comparable limiting current densities (dimensions of A cm^{-3}) when taking into account the difference in slopes. The 0.5 cm electrode, however, shows a higher current density at the limiting current for all rotation speeds studied. Figure 8 shows a logarithmic plot of (I_L/V_e) against rotation speed for two heights of 60 ppi RVCRCE (1.2 cm and 0.9 cm). This plot shows that the slope of the lines have not altered (both have a value of 0.63 with correlation coefficients greater than 0.995). It is also apparent that the limiting current densities are comparable for the two electrodes and may be described by the empirical equation:

$$\frac{I_L}{V_e} = 0.0025\,\omega^{0.63} \tag{17}$$

An attempt was made to correlate the data according to equation (3). To provide comparison with existing rotating electrode geometries the Reynolds number was based on the RVCRCE diameter. From hydrodynamic theory, the value of the Schmidt exponent, c may be taken to be equal to 1/3. The constants a and b may be determined with a double logarithmic plot of $Sh_d/Sc^{1/3}$ against Re. Figure 9 shows such a plot and it can be seen that the mass transport conditions to the RVCRCEs are sufficiently similar to allow the use of a single approximate correlation:

$$Sh_d = 0.44\,Re_d^{0.63}\,Sc^{1/3} \tag{18}$$

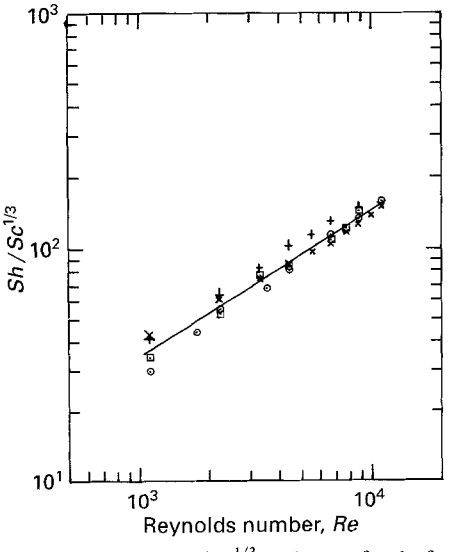

Fig. 9. Logarithmic plot of $Sh_d/Sc^{1/3}$ against Re for the four grades of rotating RVC cylinder electrode for a Reynolds number based upon the RVC cylinder diameter.

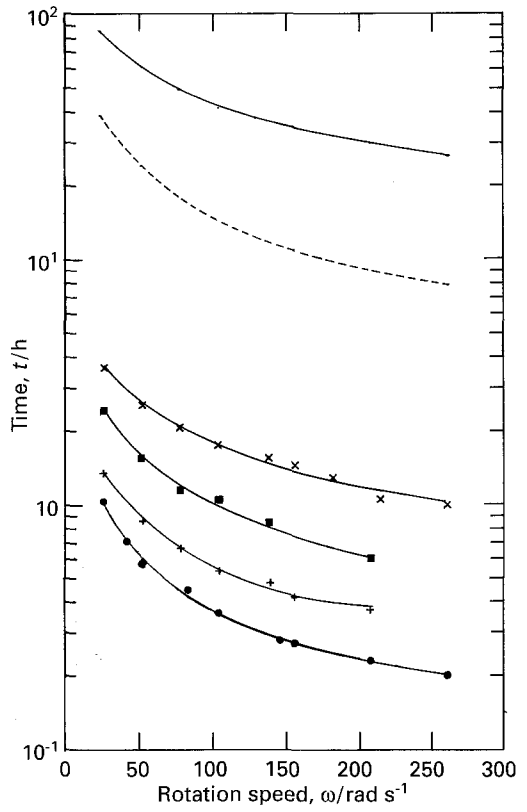

Fig. 10. Semilogarithmic plot of time for 90% copper removal against rotation speed for the four grades of rotating RVC cylinder electrode. Key: (×) 10 ppi, (■) 30 ppi, (+) 60 ppi and (●) 100 ppi. Also shown are similar plots for a smooth RDE of the same diameter and a smooth RCE of the same diameter and length. The solid and broken lines show the predicted performance for a smooth RDE having the same diameter and a smooth RCE having the same diameter and length.

High surface area electrodes have uses in, for example, controlled potential coulommetry experiments, providing more rapid reaction times when compared to the two-dimensional analogues. This property is highlighted in Fig. 10. This shows a semilogarithmic plot of time for 90% copper removal against rotation speed for the four RVCRCEs and the comparable two-dimensional analogues. The plot assumes that the system operates under complete mass transport control at 100% current efficiency and that the concentration decay for a fixed volume of electrolyte in a well mixed system follows first order behaviour according to the following equation:

$$\frac{c_t}{c_0} = \exp\left(-\frac{k_m A}{V} t\right) \qquad (19)$$

The mass transport coefficients can be considered to be similar for all four grades of rotating RVC electrodes and the graph shows the effect of electrode area on the rate of the reaction. At moderate rotation speeds (157 rad s^{-1} corresponding to 1500 rpm) the 100 ppi RVCRCE is capable of 90% copper removal from a 200 cm^3 volume of electrolyte in just over 15 min compared with approximately 30 h for the RDE under identical reaction conditions.

5. Conclusions

(i) The RVCRCEs exhibit large limiting current enhancements when compared to their two-dimensional analogues.
(ii) The mass transport coefficients to the RVCRCEs are comparable to those at a smooth RDE of the same diameter.
(iii) The limiting current enhancements are due, in the main, to the large electroactive area of the three-dimensional matrix.
(iv) The mass transport coefficients of the foams are sufficiently similar to allow the use of a single, approximate correlation based upon macroscopic electrode parameters.

Acknowledgements

This work has been supported, in part, by a Science Faculty bursary from the University of Portsmouth (to GWR). One of us (AHN) is grateful to the American University of Beirut for study leave.

References

[1] V. G. Levich, 'Physicochemical Hydrodynamics', Prentice Hall, Englewood Cliffs, NJ (1962).
[2] D. R. Gabe and F. C. Walsh, *J. Appl. Electrochem.* **13** (1983) 3.
[3] F. C. Walsh, 'The role of the rotating cylinder electrode in metal ion removal', *in* 'Electrochemistry for a Cleaner Environment', (edited by J. D. Genders and N. L. Weinberg), Electrosynthesis Co., NJ (1992) chap. 4.
[4] J. Wang, *Electrochim. Acta* **26** (1981) 1721.
[5] A. N. Strohl and D. Curran, *Anal. Chem.* **51** (1979) 353.
[6] *Idem, ibid.* **51** (1979) 1045.
[7] *Idem, ibid.* **51** (1979) 1050.
[8] J. Wang and H. Dewald, *ibid.* **55** (1983) 933.
[9] W. J. Blaedel and J. Wang, *ibid.* **52** (1980) 76.
[10] *Idem, ibid.* **52** (1980) 1697.
[11] *Idem, ibid.* **51** (1979) 1724.
[12] G. H. Heider, S. V. Sasso, K. Huang, A. M. Yacynych and H. J. Wieck, *ibid.* **62** (1990) 1106.
[13] S. Zamponi, M. Dimarino and R. J. Marassi, *Electroanal. Chem.* **248** (1989) 341.
[14] S. Zamponi, M. Berretoni and R. Marassi, *Anal. Chim. Acta* **219** (1989) 153.
[15] D. Pletcher, I. Whyte, F. C. Walsh and J. P. Millington, *J. Appl. Electrochem.* **21** (1991) 659.
[16] *Idem, ibid.* **21** (1991) 667.
[17] *Idem, ibid.* **23** (1991) 82.
[18] W. P. J. Ford, F. C. Walsh and I. Whyte, *I. Chem. E. Symp. Ser.* No. 127 (1992) 111.
[19] M. Eisenberg, C. W. Tobias and C. R. Wilke, *Chem. Eng. Prog. Symp. Ser.* No. 16 (1954) 1.
[20] Electrosynthesis Co. Inc., New Jersey, USA.
[21] C. Zhu and D. J. Curran, *Electroanalysis* **3** (1991) 511.
[22] Work in progress in the authors' laboratory.